Differential Phase Arrangement of Cellular Clocks along the Tonotopic Axis of the Mouse Cochlea Ex Vivo

Park, J.S.; Cederroth, C.R.; Basinou, V.; Sweetapple, L.; Buijink, R.; Lundkvist, G.B.; ... ; Canlon, B.

Report

Current Biology

Differential Phase Arrangement of Cellular Clocks along the Tonotopic Axis of the Mouse Cochlea Ex Vivo

Highlights

- Auditory hair cells and neurons show robust, self-sustained cellular oscillators
- PER2 oscillations are tonotopically organized in the cochlea
- Phases of cellular oscillators in the apical and middle regions differ by 3 hr
- Cochlear rhythms require potassium channels and extracellular calcium

Authors

Jung-sub Park, Christopher R. Cederroth, Vasiliki Basinou, ..., Gabriella B. Lundkvist, Stephan Michel, Barbara Canlon

Correspondence

barbara.canlon@ki.se

In Brief

Park et al. report that cochlear hair cells and neurons show robust, self-sustained cellular oscillators that are tonotopically organized and require potassium channels and calcium. The apical and middle oscillators differ in phase by 3 hr. The cellular clocks in the cochlea are dynamically regulated and longitudinally distributed.

Park et al., 2017, Current Biology *27*, 2623–2629
September 11, 2017
http://dx.doi.org/10.1016/j.cub.2017.07.019

CellPress

Current Biology
Report

Differential Phase Arrangement of Cellular Clocks along the Tonotopic Axis of the Mouse Cochlea Ex Vivo

Jung-sub Park,[1,4,6] Christopher R. Cederroth,[1,6] Vasiliki Basinou,[1,6] Lara Sweetapple,[1] Renate Buijink,[2] Gabriella B. Lundkvist,[1,3,5] Stephan Michel,[2] and Barbara Canlon[1,7,*]
[1]Department of Physiology and Pharmacology, Karolinska Institutet, 17177 Stockholm, Sweden
[2]Department of Molecular Cell Biology, Leiden University Medical Center, 2333 Leiden, the Netherlands
[3]Department of Neuroscience, Karolinska Institutet, 17177 Stockholm, Sweden
[4]Department of Otolaryngology, Ajou University School of Medicine, 164 Worldcup-ro, Yeongtong-gu, Suwon 16499, Korea
[5]Max Planck Institute for Biology of Ageing, 50931 Cologne, Germany
[6]These authors contributed equally
[7]Lead Contact
*Correspondence: barbara.canlon@ki.se
http://dx.doi.org/10.1016/j.cub.2017.07.019

SUMMARY

Topological distributions of individual cellular clocks have not been demonstrated in peripheral organs. The cochlea displays circadian patterns of core clock gene expression [1, 2]. PER2 protein is expressed in the hair cells and spiral ganglion neurons of the cochlea in the spiral ganglion neurons [1]. To investigate the topological organization of cellular oscillators in the cochlea, we recorded circadian rhythms from mouse cochlear explants using highly sensitive real-time tracking of PER2::LUC bioluminescence. Here, we show cell-autonomous and self-sustained oscillations originating from hair cells and spiral ganglion neurons. Multi-phased cellular clocks were arranged along the length of the cochlea with oscillations initiating at the apex (low-frequency region) and traveling toward the base (high-frequency region). Phase differences of 3 hr were found between cellular oscillators in the apical and middle regions and from isolated individual cochlear regions, indicating that cellular networks organize the rhythms along the tonotopic axis. This is the first demonstration of a spatiotemporal arrangement of circadian clocks at the cellular level in a peripheral organ. Cochlear rhythms were disrupted in the presence of either voltage-gated potassium channel blocker (TEA) or extracellular calcium chelator (BAPTA), demonstrating that multiple types of ion channels contribute to the maintenance of coherent rhythms. In contrast, preventing action potentials with tetrodotoxin (TTX) or interfering with cell-to-cell communication the broad-spectrum gap junction blocker (CBX [carbenoxolone]) had no influence on cochlear rhythms. These findings highlight a dynamic regulation and longitudinal distribution of cellular clocks in the cochlea.

RESULTS

Robust Cell-Autonomous PER2::LUC Rhythms in the Cochlea

Using a bioluminescence imaging system, the spatial distribution of cochlear PER2 rhythms was captured (see STAR Methods for details). Clear bioluminescence signals appeared in the cochlea ex vivo preparation (Figure S1). Signal intensity analysis of thirteen randomly chosen regions of interest (ROIs) (approximately 20–60 cells) revealed overt oscillations with a period of ~24 hr (24.63 ± 1.07; mean ± SD; n = 3 cochleae; Figure 1A, top). Visual examination of the cochlear explant, at the onset of recording, confirmed that the PER2 bioluminescence was originating from hair cells and spiral ganglion neurons, corresponding to the previously reported PER2 protein expression in the cochlea [1]. Corroborating the whole cochlear oscillations [1], the peak PER2 expression appeared in the subjective night (Figure 1B) and reached the trough in the subjective day (Figure 1C). Individual ROIs showed variable peak and trough phases, which indicated large heterogeneity across the preparation. During the second circadian cycle (24–48 hr), the total luminescence intensity peaked at 32 hr after the beginning of recordings with a peak range of 29–38 hr (Figure 1A). By visual analysis of the image series, the luminescence signals first appeared in the apex and then spread toward the middle turn of the cochlea, suggesting a longitudinal gradient of PER2 rhythms (Movie S1).

Longitudinal Arrangement of Cell Oscillators in the Cochlea

We next determined the dynamics of PER2 rhythms at the single-cell level and found that 67% of PER2::LUC-expressing cells displayed robust circadian oscillations (293 out of 438 cells from 5 different preparations; Figures 1D–1F). Representative heatmaps (Figure 1D) and oscillation curves (Figure 1E) obtained from 3 different preparations over a period of 72 hr show that the peak time of the PER2::LUC expression was variable between different cells as demonstrated across various cycles (Figure 1E). Quantification of peak-time expression during the second cycle revealed that 67% of the oscillating cells were peaking between

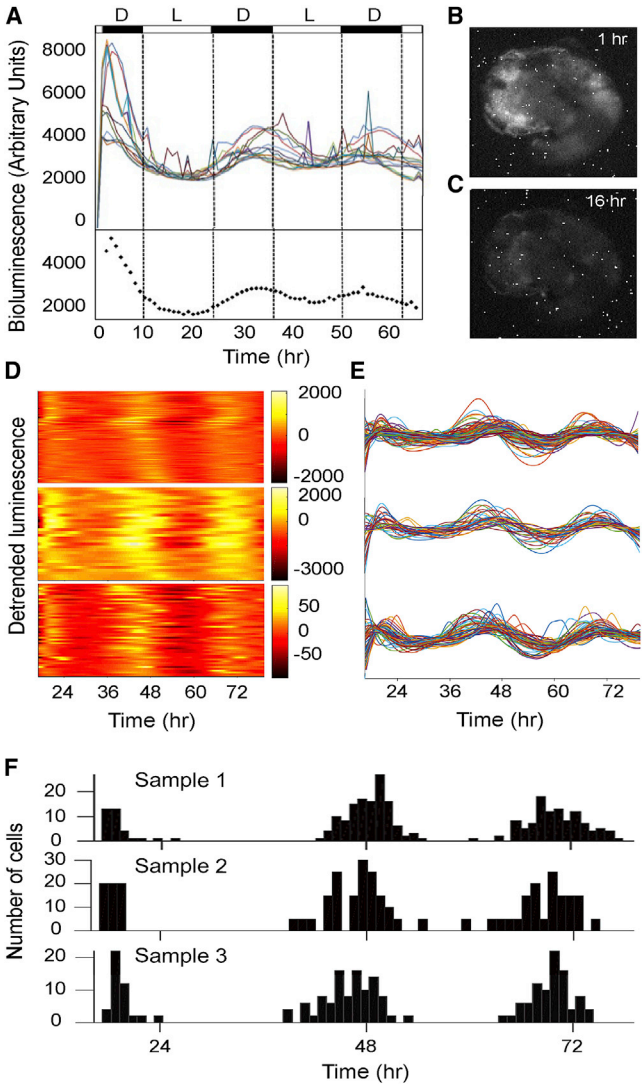

Figure 1. Robust Cell-Autonomous PER2::LUC Rhythms in the Cochlea

(A) Top: temporal changes of bioluminescence intensity in 13 different regions of interest (ROIs) within a cochlear preparation. Bottom: the dotted line shows the average bioluminescence intensity. The black and white bars above the figure indicate the light (L) and dark (D) periods of the day, respectively.

(B) Bioluminescence image of the cochlea preparation after 1 hr of recording (17:00 local time), corresponding to the peak PER2 expression.

(C) Bioluminescence image of the cochlea preparation after 16 hr of recording (08:00 local time), corresponding to the trough PER2 expression.

(D–F) Bioluminescence imaging and single-unit analysis of circadian rhythms in 3 representative samples revealed circadian patterns of PER2 expression. (D) Heatmap showing peak (yellow) and trough (orange) luminescence intensity throughout the circadian cycle over 72 hr of recordings. (E) Line plots of individual cell oscillators within the preparation. Each individual oscillator is depicted with a different color. (F) Distributions of peak expression time in the three circadian cycles that were recorded.

The scale bar represents 200 μm for (B) and (C). See also Figure S1 and Movie S1.

36 and 48 hr and 33% between 48 and 60 hr (Figure 1F). Similar peak-time variations were observed on the first and third circadian cycles (Figure 1F). Together with the time-lapsed movie showing a longitudinal PER2 wave, the peak time variation suggested that there could be a gradient of PER 2 rhythms along the tonotopic axis of the cochlea.

We then examined the oscillating profiles of cells located either in the apical or the middle regions, corresponding to low- and high-frequency sounds, respectively, that were localized in the same focal plane (Figure 2A). Bioluminescence could not be captured from the base region on the same preparation. Quantification of phase showed a significant phase delay of 2.8 hr in cells of the middle turn compared to the apical turn ($p < 0.001$; Figure 2B). Phase differences were apparent between apical and middle regions at 48 hr shown in Figures 2C and 2D. The apical population had an average phase of 44.78 ± 2.11 hr with 87.5% of the cells peaking between 36 and 48 hr and 14.28% of the cells peaking between 48 and 60 hr (Figure 2E; n = 56 cells). The middle turn population had an average phase of 47.58 ± 1.95 hr with 38.89% of the cells peaking between 36 and 48 hr and 61.11% of the cells peaking between 48 and 60 hr (Figure 2E; n = 36 cells). Such apical to middle turn differences were also observed from comparisons in different ROIs (apical turn: 28.09 ± 2.77 hr from the start of recording, mean ± SD, n = 11; middle turn: 31.56 ± 4.93 hr from the start of recording, mean ± SD, n = 9 ROI; p = 0.042).

The Apical Turn Does Not Drive the Cochlear Rhythms

Whether the apical region is required for the generation of the circadian oscillations in the cochlea was tested using a high-throughput photon-counting photomultiplier that captures whole-organ bioluminescence. Removing only the apical turn of cochlear explants, we found that the lack of apical input did not affect the phase or the period of PER2::LUC rhythms, suggesting that the apical turn does not drive cochlear rhythms (phase: 41.34 ± 1.49 hr compared to the intact cochlea 41.93 ± 1.35, mean ± SD, n = 4, p = 0.31; period: 24.37 ± 0.2 hr compared to the intact cochlea 24.27 ± 0.25, mean ± SD, n = 4, p = 0.27 by a t test). Rather, we hypothesized that the cochlea contains differentially phased cellular networks that integrate into a stable cochlear rhythm. We therefore explored this possibility by measuring the oscillations of the isolated cochlear regions (apical, middle, and basal) recorded simultaneously (Figure 3A). The amplitude of the individual regions was significantly lower than the amplitude of the whole cochlea, due to the lesser amount of tissue, but circadian PER2 rhythms were still clearly detected (Figure 3B). In the middle turn, a phase delay of 3.26 hr was found compared to the apical turn, corroborating the findings obtained from cellular recordings (Figure 2). The phase of the middle region was also delayed by 3.49 hr compared to the whole cochlea ($p < 0.001$; n = 11–13; Figure 3C). In addition, the period of the middle turn was longer than the apical turn or the whole cochlea ($p < 0.001$ for both comparisons; n = 7–10; Figure 3D). The basal part also showed some differences in phase and period when compared to the whole cochlea (phase: p = 0.047, n = 11–13; period: p = 0.024, n = 7–10; Figures 3C and 3D). Thus, multiphased cellular oscillators are organized in region-specific networks that have different degrees of synchrony along the cochlea. These findings suggest that the coupling between the different regions is required for an integrated and coherent circadian rhythm in the cochlea.

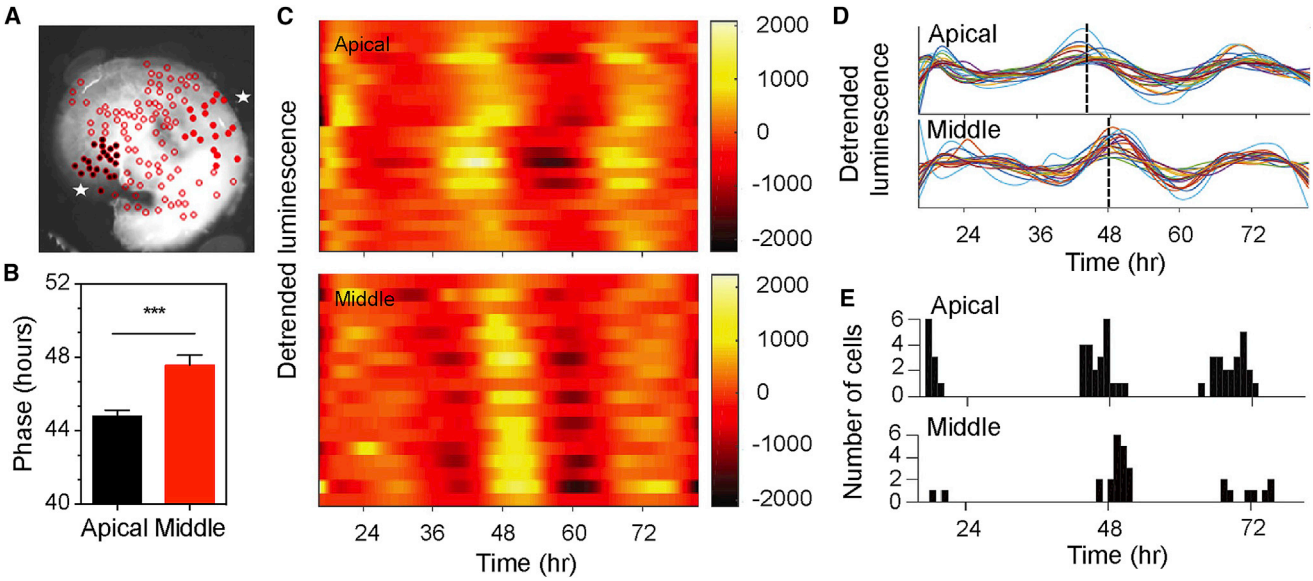

Figure 2. Tonotopical Arrangement of Circadian Cell Rhythms in the Cochlea

Temporal changes in bioluminescence monitored in individual cells located in the apical and middle cochlear regions.

(A) Bioluminescence image of the cochlea preparation from the apical and middle regions as indicated by asterisks. The selection of cell populations is shown with black full circles for the apical turn and red full circles for the middle turn. Open circles indicate cells that were not analyzed.

(B) Quantification of PER2::LUC phase in the apical and middle turn cell populations from 3 different preparations (mean ± SEM; n = 36–56 cells; ***$p < 0.001$ by t test).

(C) Representative heatmaps of apical and middle cell populations, showing peak (yellow) and trough (orange) luminescence intensity throughout the circadian cycle over 72 hr of recordings.

(D) Line plots of individual cell oscillators in apical and middle turn. The dashed lines indicate average peak phase time in the apical and middle regions.

(E) Distribution of peak time in each circadian cycle of recordings.

The scale bar represents 200 μm for (A).

Potassium and Calcium Channels Are Required for the Maintenance of Cochlear Rhythms

To determine whether intercellular communication was required for the integration of these cellular responses, we treated explants with either a voltage-gated sodium channel blocker (tetrodotoxin [TTX]; Figure 4B), an extracellular calcium chelator (1,2-Bis(2-aminophenoxy)ethane- N,N,N′,N′-tetraacetic acid [BAPTA]; Figure 4C), or a voltage-dependent potassium channel blocker (tetraethylammonium [TEA]; Figure 4D). The data showed a rapid dampening of oscillations after BAPTA and TEA treatment for 48 hr, whereas TTX did not have any effect compared to controls. Withdrawal of BAPTA or TEA resulted in the restoration of PER2::LUC oscillations, with an amplitude not differing from pretreatment samples (BAPTA, $p = 0.378$; TEA, $p = 0.109$; by t test; Figure 4E), suggesting that dampening of cochlear rhythms requires potassium and calcium transmembrane fluxes.

DISCUSSION

Using bioluminescence imaging to determine the endogenous cochlear PER2 rhythms, we were able to detect robust self-sustained cellular oscillators and found a longitudinal distribution of PER2 rhythms along the cochlear tonotopic axis. To our knowledge, this is the first peripheral organ demonstrating a spatiotemporal arrangement of cellular rhythms. Different cell types in the retina have been shown to have different phases, but how they are coordinated has not been demonstrated [3]. In the cochlea, tonotopy is a characteristic feature that allows frequency selectivity [4–6]. The mechanical isolation of the apical, middle, and basal regions show that whole-cochlear synchronicity depends on an integrated interregional communication. A spatiotemporal organization has been reported for the suprachiasmatic nucleus (SCN), where the expression of *Per1* rhythms peaks earlier in the dorsomedial part compared to the ventrolateral part [7, 8]. However, removal of the dorsal part of the SCN did not affect the synchronization of the ventral oscillators [8]. Overall, the integration of signals from the different cochlear regions appears to be required to generate a coherent synchrony of rhythms at the organ level. The physiological significance of having cellular clocks in the cochlea with different peak expression times may be related to a time-dependent regulation of frequency sensitivity, as found for spontaneous otoacoustic emissions in humans [9]. It may also be to distribute, in a time-dependent manner, energy expenses throughout the organ in order to avoid metabolic exhaustion. We have previously shown that the presence of a clock in the cochlea is associated with a differential susceptibility to noise between day and night in mice [1]. The presence of a tonotopic arrangement of cellular clocks could imply that the day/night sensitivity to noise trauma is frequency specific.

Measuring bioluminescence of reporter clock genes or their protein products in ex vivo organ cultures has been a well-established approach to investigate the function of peripheral

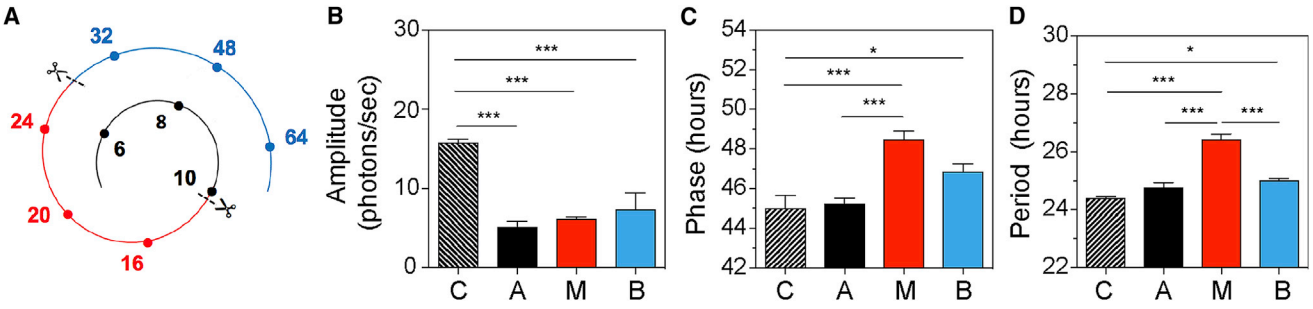

Figure 3. Contribution of the Three Cochlear Regions in the Generation of Cochlear PER2 Rhythms

(A) Frequency regions selected for PER2::LUC monitoring are depicted (black, apical turn; blue, basal turn; red, middle turn). Scissors indicate the areas where the cochlea was cut, and the numbers represent the corresponding frequencies along the tonotopic axis (kHz).

(B–D) Amplitude (B), phase (C), and period (D) of PER2::LUC rhythms in the three different cochlear regions as depicted in the diagram (A, apical turn; B, basal turn; C, whole cochlea; M, middle turn). The color of each histogram corresponds to the frequency region shown in (A). The results are presented as mean ± SEM; n = 7–13 cochleae; *p < 0.05; ***p < 0.001.

circadian clocks [10, 11]. It is known that organ-specific rhythms emerge from individual cellular oscillators. Whereas the properties of the circadian clock have been well described in isolated fibroblasts [12], in situ analysis of cellular oscillators is more challenging, due to the demand for high-amplitude bioluminescence signals. Cellular oscillators have been described in bone and tendon explants [13] as well as in the olfactory bulb, lateral habenula, arcuate nucleus, dorsomedial hypothalamus, bed nucleus of the stria terminalis, amygdala, periaqueductal gray [14–17], and retina [3]. However, to our knowledge, how cellular oscillators in peripheral tissues are organized has not been described. The current understanding of the architecture of cellular networks within tissues derives mainly from studies of the central circadian clock, the SCN, which identified a spatial arrangement of differentially phased individual SCN clocks [8, 18]. It is not fully understood how the SCN maintains synchrony, but several mechanisms have been proposed, including intercellular coupling, synaptic transmission, paracrine signaling [19, 20], and astrocyte activation [21, 22]. Furthermore, phase shift studies have demonstrated that clock gene expressions in different regions within the rat SCN readjust with different rates [7, 23–25]. Single cells in SCN brain slices from *mPer1*::*luc* transgenic mice were rhythmic; however, in the presence of TTX, the cellular oscillations were immediately lost, demonstrating that cellular communication and electrical activity are essential for circadian rhythmicity [8]. In contrast, this was not observed in the TTX-treated cochlea, suggesting that synchronization of cochlear rhythms does not require Na^{2+}-dependent action potentials.

In the retina, PER2::LUC rhythms do not require communication via melatonin, glutamate, sodium-dependent action potentials, or cx36-containing gap junctions [26]. However, dopamine and GABA immediately impaired PER2::LUC rhythms in the retina via D1, $GABA_A$, and $GABA_C$ receptors, respectively [26]. Alternative routes of intercellular communication within the cochlear epithelium include connexin-dependent Ca^{2+} wave propagation [27]. Our results buffering extracellular Ca^{2+} with BAPTA indeed indicate that a transmembrane Ca^{2+} flux or mechanotransduction processes are required for cellular rhythms or their temporal coordination [28–30]. The reduction of calcium flux has been shown to act on PER2 rhythms in the SCN [19] and could have similar actions in the cochlea. It is also possible that removing extracellular Ca^{2+} will simply disrupt intercellular junctions in the cochlear tissue [31]. Restoring normal levels of extracellular Ca^{2+}, however, led to a swift and full recovery of PER2 rhythmicity, which may be an unlikely result after structural damage. In addition, the cellular circadian clocks also depend on intrinsic properties, like membrane receptors or ion channel activation [32, 33]. Using TEA as a broadband K^+ channel antagonist has been shown to reduce cochlear action potentials, block delayed rectified K^+ currents, as well as blocking nicotinic cholinergic receptors, confirming that multiple targets could be affected [34–36]. Application of TEA to SCN neurons has been found to abolish day/night differences in membrane properties [37]. Genetic manipulation of neuronal activity in *Drosophila* clock neurons [38] or reducing SCN neuronal activity by lowering extracellular K^+ [19] results in blunted rhythms of clock genes. Our results show an impairment of cochlear PER2 rhythms under TEA treatment, suggesting that membrane excitability is also required for the maintenance of cochlear PER2 oscillations.

Organotypic cultures from a variety of tissues have been performed for the monitoring of PER2::LUC rhythms; however, histology has seldom been reported. The adult cochlea is notoriously difficult to preserve in culture, with hair cells being extremely sensitive to in vitro conditions. We found that hair cells persisted until day 3 of culture yet reduced in number (Figure S2). By day 7 of culture, very few hair cells remained, whereas spiral ganglion neurons were maintained. We thus believe that the oscillations recorded at the single-cell level (2 days in culture) reflected signals from both hair cells and spiral ganglion neurons, whereas the long-term monitoring for testing the different pharmacological agents is most likely emerging spiral ganglion neurons. The fact that PER2::LUC signals can be detected from the cochlea up to 7 days and can be reset by either a serum change (Figure 4), dexamethasone [1], or forskolin (data not shown), is a strong indication that the circadian signals obtained from the auditory neurons are extremely robust. It is therefore likely that TEA and BAPTA are affecting spiral ganglion neurons. How these communicate between each other and are affected by TEA and BAPTA remains to be clarified.

Given the broad expression pattern of the large number of heterogeneous ion channels within the cochlea [39], further studies

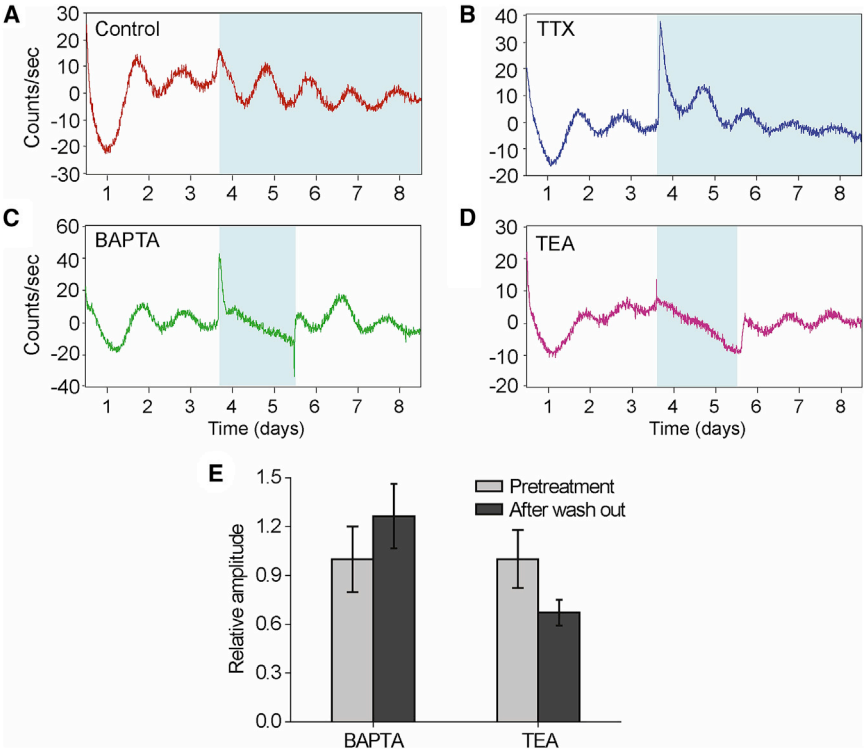

Figure 4. Contribution of Various Types of Ion Channels in the Generation of Cochlear PER2 Rhythms

(A–D) Disappearance of cochlear PER2::LUC rhythms after BAPTA or TEA treatment with re-establishment of the oscillatory activity after washout. Cochlear explants were treated with BAPTA (4 mM; C) or TEA (25 mM; D) for a period of 2 days (blue shading) and then the culture medium was replaced by fresh medium. For cochlear explants treated with vehicle (A) or TTX (40 μM; B), the culture medium was not replaced by fresh medium for a period of 5 days (blue shading).

(E) Comparison of amplitudes of pre- and post-treatment. The results are presented as mean ± SEM; n = 4–11 cochleae.

See also Figure S2.

are needed to identify the site and type of channel mediating synaptic communication between individual cellular oscillators to compose intercellular synchrony and rhythmicity in the cochlea. The dependency of PER2 rhythms on K^+ channel function and transmembrane Ca^{2+} flux indicates that these ions contribute to the self-sustained cochlear rhythms. It is well known that the cochlea relies on gap-junction coupling to maintain auditory function (for example, connexin 26, 29, 30, and 43) [40]. Our pilot experiments using carbenoxolone (CBX), a broad gap-junction inhibitor, showed no effects on the amplitude of the cochlear PER2::LUC oscillations. However, it should be noted that CBX has other targets beyond gap junctions, making interpretations difficult.

In conclusion, bioluminescence imaging and manipulating ion channels allowed us to elucidate a mechanism of cellular communication within the cochlear clock network, and these results establish a foundation for understanding how the homeostasis in the peripheral auditory system is maintained. These novel findings reveal that the cochlea possesses a spatial arrangement of cellular clocks that require transmembrane Ca^{2+} flux and K^+ channel functionality. The identification of the longitudinal organization of circadian rhythms adds another feature to the tonotopic properties of the cochlea, including neurotrophins, ion channels, and frequency tuning. Future studies aiming to uncover the circadian nature of intercellular communication within the cochlea will provide important insight of the signals needed to sustain spatiotemporal order across the organ.

STAR★METHODS

Detailed methods are provided in the online version of this paper and include the following:

SUPPLEMENTAL INFORMATION

Supplemental Information includes two figures and one movie and can be found with this article online at http://dx.doi.org/10.1016/j.cub.2017.07.019.

AUTHOR CONTRIBUTIONS

B.C., C.R.C., J.P., V.B., S.M., and G.B.L. designed the research. J.P., C.R.C., B.C., V.B., L.S., and R.B. performed research. B.C., J.P., C.R.C., V.B., R.B., L.S., and S.M. analyzed data. B.C., J.P., C.R.C., and V.B. wrote the manuscript.

ACKNOWLEDGMENTS

We thank Karima Chergui, Christian Broberger, and Håkan Westerblad for sharing reagents and Tony Jimenez-Beristain for technical support and maintenance of the PER2::LUC colony. This work was supported by Swedish Medical Research Council grant K2014-99X-22478-01-3 (to B.C.), National Institute on Deafness and Other Communication Disorders of the NIH grant R21DC013172 (to B.C.), National Research Foundation of Korea grant 2014R1A6A3A03058661 funded by the Ministry of Education of the Korean Government (to J.P.), the Karolinska Institutet (to B.C. and C.R.C.), Tysta Skolan (to B.C., J.P., C.R.C., and G.B.L), Lars Hiertas Minne (to C.R.C.), Magnus Bergvalls (to C.R.C.), and Karolinska Institutet HÖST (Hearing, Otolaryngology, Language and Speech) (to V.B.).

Received: April 21, 2017
Revised: June 15, 2017
Accepted: July 7, 2017
Published: August 17, 2017

REFERENCES

1. Meltser, I., Cederroth, C.R., Basinou, V., Savelyev, S., Lundkvist, G.S., and Canlon, B. (2014). TrkB-mediated protection against circadian sensitivity to noise trauma in the murine cochlea. Curr. Biol. *24*, 658–663.
2. Basinou, V., Park, J.S., Cederroth, C.R., and Canlon, B. (2017). Circadian regulation of auditory function. Hear. Res. *347*, 47–55.
3. Besharse, J.C., and McMahon, D.G. (2016). The retina and other light-sensitive ocular clocks. J. Biol. Rhythms *31*, 223–243.
4. Rosenblatt, K.P., Sun, Z.-P., Heller, S., and Hudspeth, A.J. (1997). Distribution of Ca2+-activated K+ channel isoforms along the tonotopic gradient of the chicken's cochlea. Neuron *19*, 1061–1075.
5. Davis, R.L. (2003). Gradients of neurotrophins, ion channels, and tuning in the cochlea. Neuroscientist *9*, 311–316.
6. Ricci, A.J., Crawford, A.C., and Fettiplace, R. (2003). Tonotopic variation in the conductance of the hair cell mechanotransducer channel. Neuron *40*, 983–990.
7. Nakamura, W., Yamazaki, S., Takasu, N.N., Mishima, K., and Block, G.D. (2005). Differential response of Period 1 expression within the suprachiasmatic nucleus. J. Neurosci. *25*, 5481–5487.
8. Yamaguchi, S., Isejima, H., Matsuo, T., Okura, R., Yagita, K., Kobayashi, M., and Okamura, H. (2003). Synchronization of cellular clocks in the suprachiasmatic nucleus. Science *302*, 1408–1412.
9. Haggerty, H.S., Lusted, H.S., and Morton, S.C. (1993). Statistical quantification of 24-hour and monthly variabilities of spontaneous otoacoustic emission frequency in humans. Hear. Res. *70*, 31–49.
10. Yoo, S.H., Yamazaki, S., Lowrey, P.L., Shimomura, K., Ko, C.H., Buhr, E.D., Siepka, S.M., Hong, H.K., Oh, W.J., Yoo, O.J., et al. (2004). PERIOD2:LUCIFERASE real-time reporting of circadian dynamics reveals persistent circadian oscillations in mouse peripheral tissues. Proc. Natl. Acad. Sci. USA *101*, 5339–5346.
11. Abraham, U., Prior, J.L., Granados-Fuentes, D., Piwnica-Worms, D.R., and Herzog, E.D. (2005). Independent circadian oscillations of Period1 in specific brain areas in vivo and in vitro. J. Neurosci. *25*, 8620–8626.
12. Welsh, D.K., Yoo, S.-H., Liu, A.C., Takahashi, J.S., and Kay, S.A. (2004). Bioluminescence imaging of individual fibroblasts reveals persistent, independently phased circadian rhythms of clock gene expression. Curr. Biol. *14*, 2289–2295.
13. Lande-Diner, L., Stewart-Ornstein, J., Weitz, C.J., and Lahav, G. (2015). Single-cell analysis of circadian dynamics in tissue explants. Mol. Biol. Cell *26*, 3940–3945.
14. Guilding, C., Hughes, A.T., Brown, T.M., Namvar, S., and Piggins, H.D. (2009). A riot of rhythms: neuronal and glial circadian oscillators in the mediobasal hypothalamus. Mol. Brain *2*, 28.
15. Guilding, C., Hughes, A.T.L., and Piggins, H.D. (2010). Circadian oscillators in the epithalamus. Neuroscience *169*, 1630–1639.
16. Landgraf, D., Long, J.E., and Welsh, D.K. (2016). Depression-like behaviour in mice is associated with disrupted circadian rhythms in nucleus accumbens and periaqueductal grey. Eur. J. Neurosci. *43*, 1309–1320.
17. Guilding, C., and Piggins, H.D. (2007). Challenging the omnipotence of the suprachiasmatic timekeeper: are circadian oscillators present throughout the mammalian brain? Eur. J. Neurosci. *25*, 3195–3216.
18. Evans, J.A. (2016). Collective timekeeping among cells of the master circadian clock. J. Endocrinol. *230*, R27–R49.
19. Lundkvist, G.B., Kwak, Y., Davis, E.K., Tei, H., and Block, G.D. (2005). A calcium flux is required for circadian rhythm generation in mammalian pacemaker neurons. J. Neurosci. *25*, 7682–7686.
20. Mohawk, J.A., Green, C.B., and Takahashi, J.S. (2012). Central and peripheral circadian clocks in mammals. Annu. Rev. Neurosci. *35*, 445–462.
21. Brancaccio, M., Patton, A.P., Chesham, J.E., Maywood, E.S., and Hastings, M.H. (2017). Astrocytes control circadian timekeeping in the suprachiasmatic nucleus via glutamatergic signaling. Neuron *93*, 1420–1435.e5.
22. Tso, C.F., Simon, T., Greenlaw, A.C., Puri, T., Mieda, M., and Herzog, E.D. (2017). Astrocytes regulate daily rhythms in the suprachiasmatic nucleus and behavior. Curr. Biol. *27*, 1055–1061.
23. Yamazaki, S., and Takahashi, J.S. (2005). Real-time luminescence reporting of circadian gene expression in mammals. Methods Enzymol. *393*, 288–301.
24. Nagano, M., Adachi, A., Nakahama, K., Nakamura, T., Tamada, M., Meyer-Bernstein, E., Sehgal, A., and Shigeyoshi, Y. (2003). An abrupt shift in the day/night cycle causes desynchrony in the mammalian circadian center. J. Neurosci. *23*, 6141–6151.
25. Albus, H., Vansteensel, M.J., Michel, S., Block, G.D., and Meijer, J.H. (2005). A GABAergic mechanism is necessary for coupling dissociable ventral and dorsal regional oscillators within the circadian clock. Curr. Biol. *15*, 886–893.
26. Ruan, G.X., Allen, G.C., Yamazaki, S., and McMahon, D.G. (2008). An autonomous circadian clock in the inner mouse retina regulated by dopamine and GABA. PLoS Biol. *6*, e249.
27. Anselmi, F., Hernandez, V.H., Crispino, G., Seydel, A., Ortolano, S., Roper, S.D., Kessaris, N., Richardson, W., Rickheit, G., Filippov, M.A., et al. (2008). ATP release through connexin hemichannels and gap junction transfer of second messengers propagate Ca2+ signals across the inner ear. Proc. Natl. Acad. Sci. USA *105*, 18770–18775.
28. Johnson, S.L., Forge, A., Knipper, M., Münkner, S., and Marcotti, W. (2008). Tonotopic variation in the calcium dependence of neurotransmitter release and vesicle pool replenishment at mammalian auditory ribbon synapses. J. Neurosci. *28*, 7670–7678.
29. Cho, S., and von Gersdorff, H. (2014). Proton-mediated block of Ca2+ channels during multivesicular release regulates short-term plasticity at an auditory hair cell synapse. J. Neurosci. *34*, 15877–15887.
30. Corns, L.F., Johnson, S.L., Kros, C.J., and Marcotti, W. (2014). Calcium entry into stereocilia drives adaptation of the mechanoelectrical transducer current of mammalian cochlear hair cells. Proc. Natl. Acad. Sci. USA *111*, 14918–14923.
31. Mammano, F., and Bortolozzi, M. (2017). Ca^{2+} signaling, apoptosis and autophagy in the developing cochlea: milestones to hearing acquisition. Cell Calcium. Published online May 11, 2017. http://dx.doi.org/10.1016/j.ceca.2017.05.006.
32. Allen, C.N., Nitabach, M.N., and Colwell, C.S. (2017). Membrane currents, gene expression, and circadian clocks. Cold Spring Harb. Perspect. Biol. *9*, a027714.
33. Colwell, C.S. (2011). Linking neural activity and molecular oscillations in the SCN. Nat. Rev. Neurosci. *12*, 553–569.
34. Marcotti, W., Johnson, S.L., and Kros, C.J. (2004). Effects of intracellular stores and extracellular Ca(2+) on Ca(2+)-activated K(+) currents in mature mouse inner hair cells. J. Physiol. *557*, 613–633.
35. Dawkins, R., and Sewell, W.F. (2004). Afferent synaptic transmission in a hair cell organ: pharmacological and physiological analysis of the role of the extended refractory period. J. Neurophysiol. *92*, 1105–1115.
36. Blanchet, C., and Dulon, D. (2001). Tetraethylammonium ions block the nicotinic cholinergic receptors of cochlear outer hair cells. Brain Res. *915*, 11–17.
37. Kuhlman, S.J., and McMahon, D.G. (2004). Rhythmic regulation of membrane potential and potassium current persists in SCN neurons in the absence of environmental input. Eur. J. Neurosci. *20*, 1113–1117.
38. Nitabach, M.N., Blau, J., and Holmes, T.C. (2002). Electrical silencing of Drosophila pacemaker neurons stops the free-running circadian clock. Cell *109*, 485–495.
39. Reijntjes, D.O., and Pyott, S.J. (2016). The afferent signaling complex: regulation of type I spiral ganglion neuron responses in the auditory periphery. Hear. Res. *336*, 1–16.

40. Jagger, D.J., and Forge, A. (2015). Connexins and gap junctions in the inner ear–it's not just about K^+ recycling. Cell Tissue Res. *360*, 633–644.

41. Eilers, P.H. (2003). A perfect smoother. Anal. Chem. *75*, 3631–3636.

42. Savelyev, S.A., Larsson, K.C., Johansson, A.S., and Lundkvist, G.B. (2011). Slice preparation, organotypic tissue culturing and luciferase recording of clock gene activity in the suprachiasmatic nucleus. J. Vis. Exp. (48), 2439.

43. Park, J.S., Cederroth, C.R., Basinou, V., Meltser, I., Lundkvist, G., and Canlon, B. (2016). Identification of a circadian clock in the inferior colliculus and its dysregulation by noise exposure. J. Neurosci. *36*, 5509–5519.

STAR★METHODS

KEY RESOURCES TABLE

REAGENT or RESOURCE	SOURCE	IDENTIFIER
Chemicals, Peptides, and Recombinant Proteins		
D-luciferin potassium salt	Promega	Cat# E1602
Tetrodotoxin	Sigma-Aldrich	Cat#T8024
Tetraethylammonium chloride	Sigma-Aldrich	Cat#T2265
Carbenoxolone disodium salt	Sigma-Aldrich	Cat#C4790
1,2-Bis(2-aminophenoxy)ethane-N,N,N',N'-tetraacetic acid	Tocris Bioscience	Cat#2786
Experimental Models: Organisms/Strains		
Mouse: PERIOD2::LUCIFERASE transgenic mice in a C57BL/6 background	Yoo et al., 2004 [10]	N/A
Software and Algorithms		
Image Pro Plus	Media Cybernetics	http://www.mediacy.com/imageproplus
TSA toolbox	Mathworks	https://se.mathworks.com/products/matlab.html
GraphPad Prism 6	GraphPad software	https://www.graphpad.com/
X, Y, Z driver	Objective Imaging	http://www.objectiveimaging.com/OI_Oasis4i.htm
Lumicycle Analysis software	Actimetrics	http://actimetrics.com/products/lumicycle/
Other		
Millicell membrane	Millipore	PICM0RG50
Digital CCD Camera	Hamamatsu	ORCA UU-BT-1024
Microscope	Olympus	BX51WIF
Microscope lens	Olympus	10x LWD
Microscope stage	Luigs und Neumann	Luigs & Neumann XY-shifting Table 240
Micromanipulator	Märzhäuser Wetzlar	MA-42Z
Luminometer	Actimetrics	LumiCycle 32

CONTACT FOR REAGENT AND RESOURCE SHARING

Further information and requests for resources and reagents should be directed to and will be fulfilled by the Lead Contact, Barbara Canlon (barbara.canlon@ki.se).

EXPERIMENTAL MODEL AND SUBJECT DETAILS

Recordings of circadian oscillations of the PER2 protein were performed using tissues obtained from homozygotic knock-in PERIOD2::LUCIFERASE (PER2::LUC) transgenic mice with a C57BL/6 background [10], generously provided by Prof. J. Takahashi. All experimental procedures on animals were performed in accordance with the guidelines and regulations set forth by Karolinska Institutet and "Stockholm's Norra Djurförsöksetiska Nämnd," as well as the Dutch law on Animal welfare and approved by the Dutch government (DEC 11010). Animals had ad libitum access water and to food (Lactamin R34, Lantmännen). Temperature was maintained between 19°C and 21°C and lights were on at 6:00 hr and off at 18:00 hr.

METHOD DETAILS

Bioluminescence imaging for single-cell

Cochlea from male adult mice were dissected from PER2::LUC mice (4-6 weeks old) and cultured organotypically on a Millicell membrane (PICM0RG 50; Millipore, Billerica, MA). Organotypic cultures of the cochlea were prepared as described previously [1]. The cochleae were isolated and organotypic cultures were maintained on a Millicell membrane insert. Membrane inserts were placed in a sealed 35 mm dish containing 1.2 mL of Dulbecco's Modified Eagles Medium (D7777, Sigma-Aldrich) supplemented with 10 mM HEPES-buffer (Sigma-Aldrich), 2% B-27 (Thermo Fisher Scientific, Waltham, MA), 5 U/ml penicillin and 5 μg/ml streptomycin (0.1% penicillin-streptomycin, Sigma-Aldrich) and 0.2 mM D-luciferin potassium salt (Promega, Madison, WI), adjusted to pH 7.2 with NaOH. Organotypic cochlea cultures were immediately transferred to an upright microscope (BX51WIF, Olympus, Tokyo, Japan)

housed in a light tight and temperature controlled chamber 37°C (Life Imaging Services, Reinach, Switzerland). The microscope was equipped with a long-working distance objective (10x LWD, Olympus), a cooled CCD camera (ORCA UU-BT-1024, Hamamatsu, Japan) and a motorized stage (Luigs & Neumann XY-shifting Table 240) as well as focus control (Marzhauser MA-42Z) both connected to an OASIS-4i Four Axis Controller. Bioluminescence images were obtained from cochlear cultures using 60 min exposure times. Focus was adjusted to image PER2::LUC expressing cochlea cells in one focal plane. Cell-like regions were later defined in the offline analysis and followed in time. Stage and focus position as well as image acquisition were controlled by software (Image Pro Plus, Media Cybernetics, Warrendale, PA; StagePro plug-in, Objective Imaging, Cambridge, UK).

From the images, cell-like regions were selected using an in-house written program for analyzing life cell recording (stacks). For convenience we will refer to these cell-like ROIs as ''single cells.'' The luciferase signal in the hair cells were distinguished from the spiral ganglion neurons by their location. The spiral ganglion neurons are more medial. For every single cell, the average brightness was calculated in each image and the resulting time series were further analyzed using MATLAB-based (Mathworks, Natick, MA) scripts. In order to limit noise and augment the efficiency for subsequent analyses, a previously described algorithm [41] was used to smooth and resample the data to one data point per minute. This provides a sinusoid wave for each single cell. Finally, the smoothed data were detrended and normalized using a fourth order polynomial from the TSA toolbox for MATLAB. The processed intensity traces from the single cell rhythms were evaluated on sustained PER2::LUC signal and circadian rhythmicity. Single-cells were only used if the time series contains at least three viable peaks, where peaks are above the trendline and troughs are below this trendline, and the distance between the peaks is on average within the circadian range of 20-28 hr.

Organotypic cochlear explants and analysis

Cochleae were dissected from male PER2::LUC mice (4-6 weeks old) and cultured organotypically on a Millicell membrane (PICMORG 50; Millipore, Billerica, MA). Cochleae were removed from the temporal bone and placed in Hank's balanced salt solution (HBSS) buffer with supplements pH 7.2 and 285-315 mOsm/Kg. The cochleae were dissected free of the otic capsule bone and stria vascularis and then transferred to the Millicell membrane and kept in culture for minimum 6 days, as described [1]. The cochlea that was placed on the membrane contained the organ of Corti including the modiolus and were kept in culture for minimum 6 days, as described [1]. For bioluminescence imaging of the different cochlear regions, the cochlea were separated into segments (apex, middle and base), by a perpendicular cut. Cochlear explants were treated with 4 mM BAPTA (Tocris Bioscience, Bristol, UK), 25 mM TEA, 0.5 μM TTX (Sigma-Aldrich, St. Louis, MO) that were dissolved in DMEM-based culture medium, as described [42]. Real-time luciferase reporter technology was used as described previously [42, 43]. Bioluminescence recordings were done in the LumiCycle Luminometer (Actimetrics, Wilmette, IL, USA) that was placed in a 37°C incubator. Analysis of PER2::LUC rhythms (period, amplitude, and phase) was performed by fitting a sine wave to a 24h-running average after subtraction of the baseline, using the Lumicycle Analysis software (Actimetrics, Wilmette, IL, USA). The first day of measurements was excluded from the analysis. The amplitudes of whole cochlea and three different cochlear regions were calculated from 3 half-cycles (1.5 cycles), as the difference between highest (peak) and lowest (trough) photon count. For the assessment of ion channels, amplitudes were compared with the values from 3 half-cycles immediately before treatment and after washout. The very first peak after washout was excluded. Phase responses were determined as maximum (peak) luminescence between 24 and 48 hr after the start of the recording. Five consecutive peaks were used for period calculations.

QUANTIFICATION AND STATISTICAL ANALYSIS

Data are presented as mean ± SEM. Statistical analyses were performed with GraphPad Prism 6 (GraphPad software). To compare phases in the apical and middle turn cell populations and to assess amplitudes before BAPTA or TEA treatment and after washout, unpaired Student's t test was used (Figure 2B, n = 36-56 cells; Figure 4E, n = 4-11 cochleae). A one-way ANOVA was used to compare amplitude, phase and period of PER2::LUC rhythms in the three different cochlear regions (Figures 3B–3D, n = 7-13 cochleae).